Supporting information

Piezotronic-Enhanced Photoelectrochemical Reactions in $Ni(OH)_2$ Decorated ZnO Photoanodes

Hongxia Li,[1,2,‡] Yanhao Yu,[1,‡] Matthew B. Starr,[1] Zhaodong Li,[1] Xudong Wang[1,*]

1. Department of Materials Science and Engineering, University of Wisconsin-Madison

2. College of Materials and Environmental Engineering, Hangzhou Dianzi University, Hangzhou, 310018, People's Republic of China.

‡These authors contributed equally

*Email: xudong@engr.wisc.edu

S1: Experimental details

RF sputtering ZnO Film: The (001)-oriented ZnO film was deposited in a radiofrequency (RF) sputtering system. Prior to deposition, the ITO/PET substrate with a size of 1 cm × 3 cm was sequentially cleaned by ultrasonic in acetone, ethanol, and DI water and dried by N_2 gas. During the sputtering, the system pressure was maintained at pressure of 1.5×10^{-3} Torr under Ar (20 sccm) flow. The RF power for sputtering was kept at 55 W. The total deposition time was 120 min for a film thickness of ~100 nm.

Electrodeposition of $Ni(OH)_2$: $Ni(OH)_2$ film was electrodeposited onto ZnO/ITO/PET substrate in 0.05M $Ni(NO_3)_2$ solution by passing a constant cathodic current density of 0.7mA/cm^2 for 2 min. Three-electrode system was applied during the coating with Pt wire and SCE as the counter and reference electrode, respectively.

PEC cell fabrication: The PEC cell has a layered structure of PET/ITO/ZnO/$Ni(OH)_2$. The entire device was attached to a PMMA cantilever (3 cm × 20 cm), which can be deformed to produce various strains. The working area was defined to ~0.1 cm^2 by epoxy coating.

PEC measurement: Three-electrode configuration was employed to conduct PEC measurements with Pt wire and SCE as the counter and reference electrode, respectively. The PMMA cantilever with PEC device was anchored onto a home-made acrylic stage, which was fixed at the bottom of a glass beaker. The exposed PEC cell surface was located 2 cm above the fix point. Considering the much larger length (13 cm) of the cantilever beam, the strain subjected

to the active PEC area was assumed to be uniform. Under this assumption, the strain at the PEC area was calculated based on the cantilever banding theory by measuring the lateral deflection distance at the cantilever tip.[1,2] For sulfite oxidation and OER experiments, 1M Na_2SO_3 and 18.2 MΩ DI water were used as the electrolyte, respectively. The light illumination was provided by a 150 W Xenon lamp (Newport Corporation). During the measurement, all electrodes were connected to a potentiostat system (Metrohm Inc.).

Characterizations: SEM measurements were performed on Zeiss Leo 1530 field-emission microscope. TEM and FFT characterizations were conducted on FEI TF30 microscopes. XPS was acquired on a Thermo Scientific K-alpha XPS instrument. The survey range was from 0 to 1300 eV. The Ni 2p and Zn 2p spectra were individually scanned for characterizing the chemical structures of $Ni(OH)_2$ and ZnO.

S2: Supplementary figures

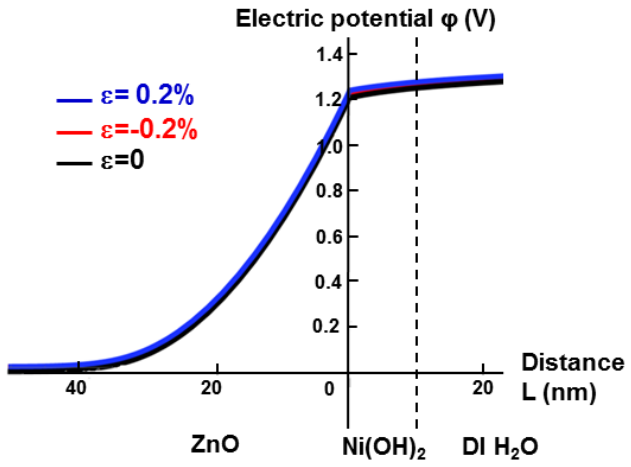

Figure S1. φ distribution of ZnO/H_2O heterojunction under different strain conditions, showing piezoelectric polarization can barely change the depletion of ZnO without $Ni(OH)_2$.

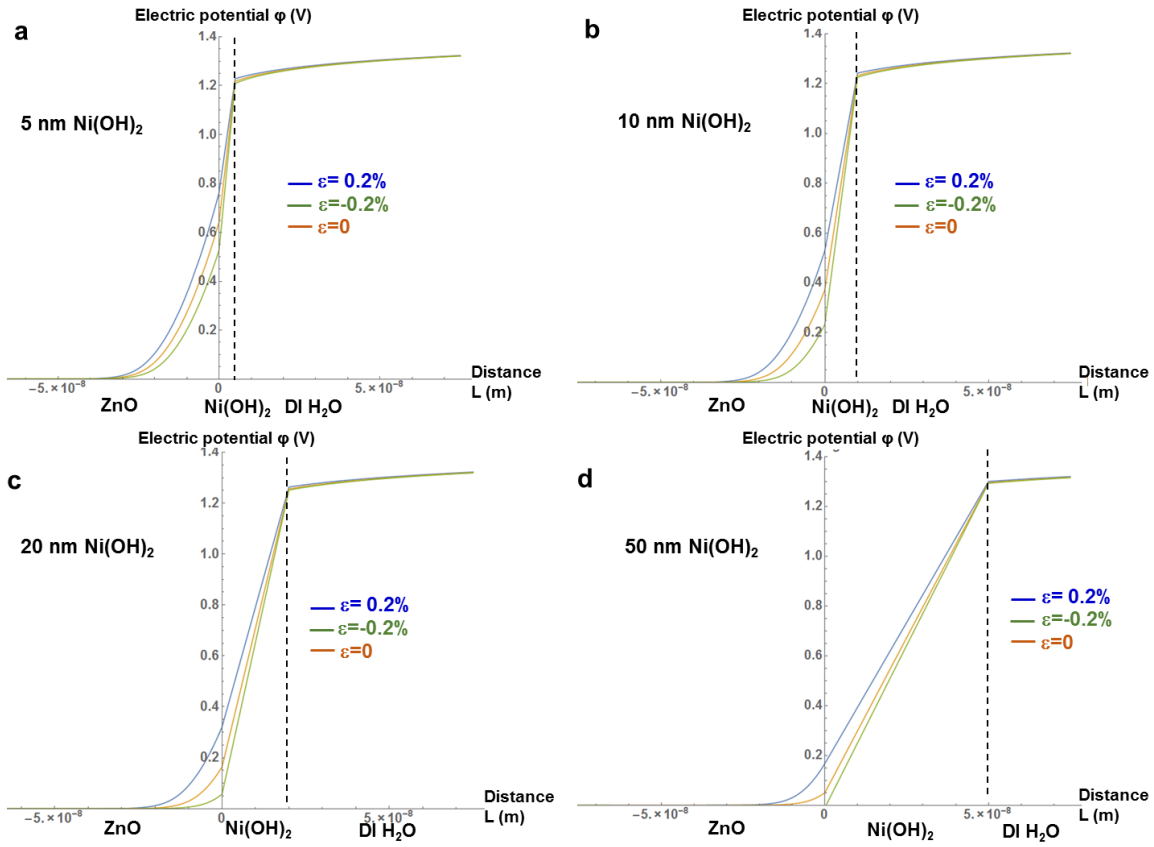

Figure S2. φ distributions of ZnO/$Ni(OH)_2$/H_2O heterojunctions with 5 nm (a), 10 nm (b), 20 nm (c) and 50 nm (d)-thick $Ni(OH)_2$ layer under different strain conditions.

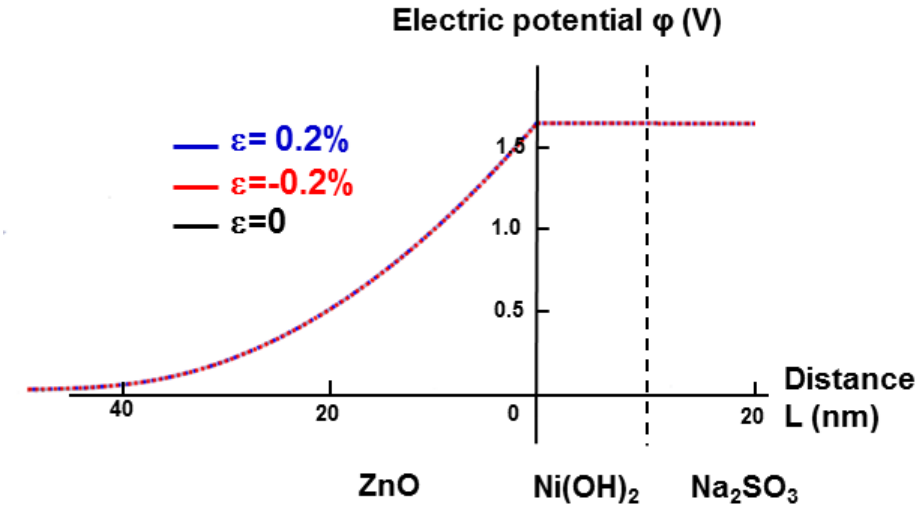

Figure S3. φ distribution of ZnO/Na_2SO_3 heterojunction under different strain conditions, showing little effect can be induced by piezoelectric polarization without $Ni(OH)_2$.

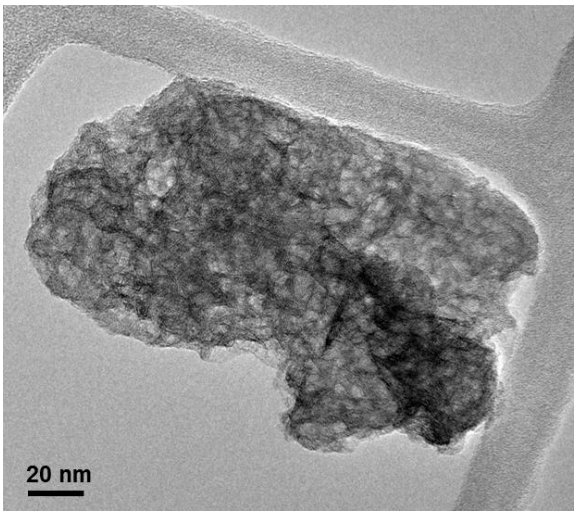

Figure S4. TEM image of an individual $Ni(OH)_2$ sheet, indicating the semitransparent feature.

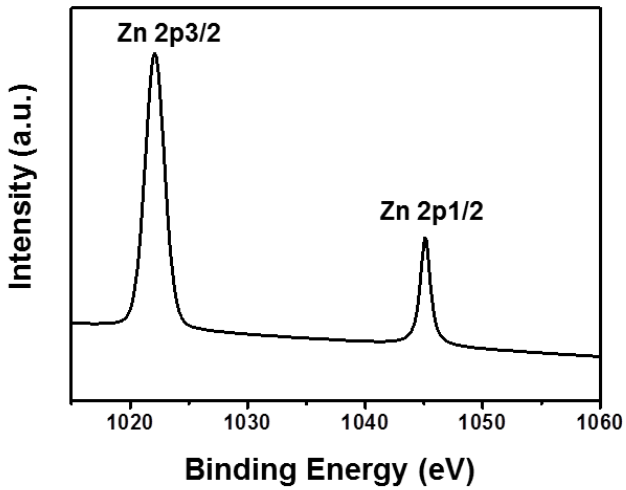

Figure S5. Zn 2p scan for $ZnO/Ni(OH)_2$ heterostructure.

S3: Calculation of electric potential profile at the $ZnO/Ni(OH)_2/H_2O$ heterojunction.

At thermodynamic equilibrium, the total electrical potential (V) change across a heterojunction (in the absence of piezoelectric charge) is equal to the total Fermi energy (E_F) difference between the materials composing the junction. It is important to emphasize that while charge conservation is always a key constraint in the system, material parameters such as electrical permittivity, free charge density, and (insulator) layer thickness can dramatically change the total amount of charge transfer necessary to create a specific magnitude of V.

Calculating the electrical potential distribution begins with an accounting of the physical properties of the materials composing the heterojunction before any charge exchange occurs (Figure S6, Table S1 at the end of the supplemental materials).

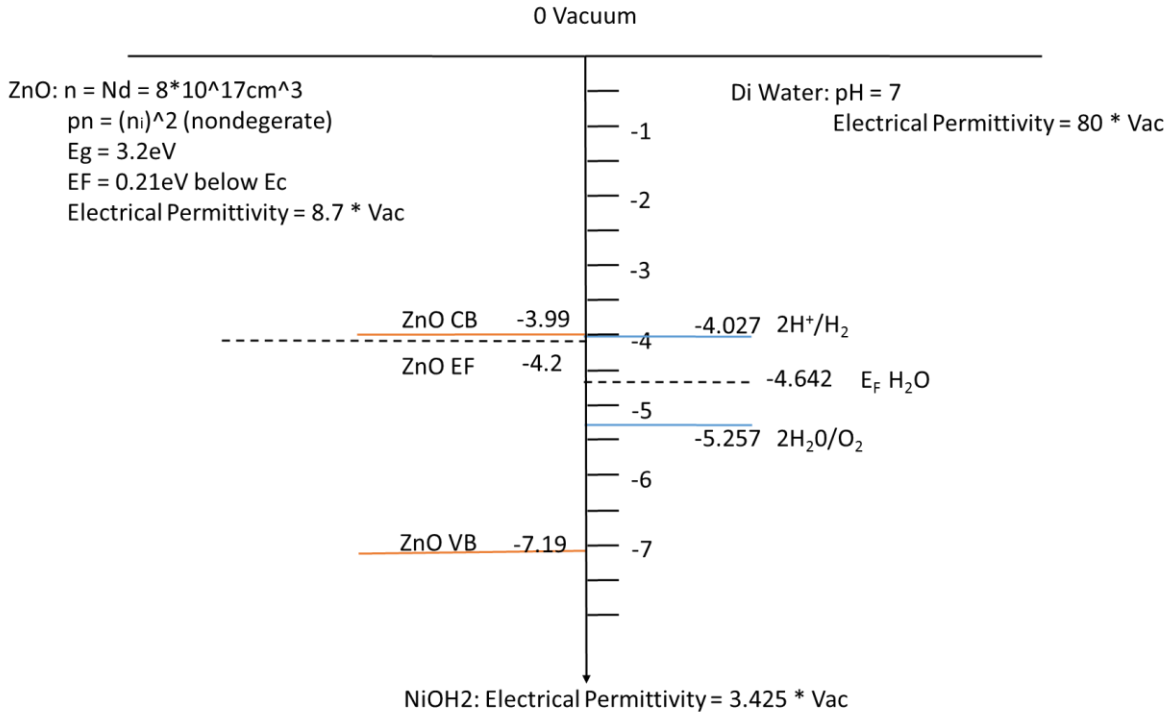

Figure S6. The relative band and Fermi energy (E_F) positions of relevant materials. Vacuum energy is chosen as a convenient universe reference. The band positions of $Ni(OH)_2$ are arbitrarily selected to exemplify the material's resistive properties.

When the materials composing the heterojunction are placed in intimate contact with one another, entropy drives charge exchange between the conductive phases (i.e. ZnO and the H_2O solution). This charge exchange continues until the imbalance of electrical charge creates an electrical potential difference between the two phases that is equal to the bulk E_F difference between the two phases. Free and bound charges in the ZnO and H_2O are pushed and pulled by the electric field (potential gradient $\frac{dV}{dx}$) this charge exchange creates, causing accumulation and depletion of charge in the vicinity of the heterojunction. These charge accumulation regions act to screen the

junction's electric field from the bulk. To understand the potential distribution in the vicinity of the heterojunction we must understand how electrical potentials effect charge distributions.

From electrostatics, the Poisson equation describes how the charge density at location x ($\rho(x)$) is influenced by the potential at location x ($V(x)$):

$$\frac{d^2V(x)}{dx^2} = \frac{-\rho(x)}{\epsilon_0\epsilon_r} \tag{S1}$$

Where ϵ_0 and ϵ_r are the electrical permittivity of vacuum and the medium inhabited by the charge, respectively. $V(x)$ is be solved for all x by twice integrating $\rho(x)$, but we first must get ρ as a function of $V(x)$.

In the ZnO semiconductor, the charge density is comprised of mobile electrons and holes as well as the immobile charged atoms that we attribute to dopant atoms:

$$\rho_{ZnO}(x) = (z_n)(n(x)) + (z_p)(p(x)) + z_d Nd_{ZnO} \tag{S2}$$

Where z_n, z_p and z_d are the charge of an electron (-1), hole (1) and dopant atom (1) in ZnO, respectively, and $n(x)$, $p(x)$ and Nd_{ZnO} are the charge density of electrons, holes, and dopant atoms, respectively.

The charge density of electrons and holes varies with position because the electrical potential (relative to bulk potential in ZnO) varies as x approaches the heterojunction.

In both semiconductors and solutions, the ratio of concentrations of charged species i in bulk (n_i^0) at bulk potential ($\varphi^0 = 0$) to its concentration (n_i) found at any other potential (φ) is taken to depend upon the Boltzmann factor in the following way:

$$n_i = n_i^0 e^{\left(\frac{-z_i e\phi(x)}{kT}\right)} \tag{S3}$$

where z_i is the charge of ion *i*, and *e* is the charge of the electron, φ is the potential relative to bulk solution, *x* is a measure of distance into solution and perpendicular to the monolayer surface, *k* is the Boltzmann constant, and *T* is absolute temperature.

Combining equation S2 and S3 results in the following expression for charge density in the semiconductor:

$$\rho_{ZnO}(x) = (z_n)(n_b)e^{\frac{(z_n)V(x)e}{kT}} + (z_p)(p_b)e^{\frac{(z_p)V(x)e}{kT}} + z_d Nd_{ZnO} \tag{S4}$$

Where n_b and p_b are the bulk concentrations of electrons and holes, respectively.

Applying this same treatment to the DI-H_2O medium, where H^+ and OH^- ions comprise the charge density, yields the following expression for the charge density in the aqueous medium:

$$\rho_{H_2O}(x) = \left(z_{H^+}\right)(H^+{}_b)e^{\frac{(z_{H^+})V(x)e}{kT}} + (z_{OH^-})(OH^-{}_b)e^{\frac{(z_{OH^-})V(x)e}{kT}} \tag{S5}$$

Where z_{H^+} and z_{OH^-} are the charge of hydronium (1) and hydroxyl (-1) ions, respectively, and ${H^+}_b$ and ${OH^-}_b$ are the bulk concentrations of hydronium and hydroxyl ions in DI-H_2O, respectively.

Equations S4 and S5 can be combined with Eq. S1 to yield the following expressions that describe how potential and charge density are interrelated in both the DI-H_2O and ZnO:

$$\text{In the Semiconductor: } \frac{d^2V}{dx^2} = \frac{-((z_n)(n_b)e^{\frac{(z_n)V(x)e}{kT}} + (z_p)(p_b)e^{\frac{(z_p)V(x)e}{kT}} + z_d Nd_{ZnO})}{\epsilon_0 \epsilon_r} \tag{S6}$$

$$\text{In the Solution: } \frac{d^2V}{dx^2} = \frac{-(\left(z_{H^+}\right)({H^+}_b)e^{\frac{(z_{H^+})V(x)e}{kT}} + \left(z_{OH^-}\right)({OH^-}_b)e^{\frac{(z_{OH^-})V(x)e}{kT}})}{\epsilon_0 \epsilon_r} \tag{S7}$$

To solve these second order differential equations requires two boundary conditions for each expression.

In the semiconductor, the boundary conditions are as follows:

1. The electric field ($\frac{dV}{dx}$) in the bulk of the ZnO is zero.
$$\left(\frac{dV}{dx}\right)_{x=-\infty} = 0 \tag{S8}$$
2. The electrical potential in the bulk is equal to the Fermi energy of ZnO ($V_{EF_{ZnO}}$)
$$V_{x=-\infty} = V_{EF_{ZnO}} \tag{S9}$$

In the solution phase, the boundary conditions are similar:

1. The electric field ($\frac{dV}{dx}$) in the bulk of DI-H_2O is zero.
$$\left(\frac{dV}{dx}\right)_{x=\infty} = 0 \tag{S10}$$
2. The electrical potential in the bulk is equal to the Fermi energy of DI-H_2O ($V_{EF_{H2O}}$).
$$V_{x=\infty} = V_{EF_{H2O}} \tag{S11}$$

Applying boundary conditions S8 and S9 to expression S6 during integration yields the following expression for the potential gradient in the ZnO:

$$\frac{dV}{dx} = \sqrt{-\frac{2kT}{\epsilon_0 \epsilon_{ZnO}}\left[\left(n_b\left[e^{\frac{z_n Ve}{kT}}\right] - 1\right) + \left(p_b\left[e^{\frac{z_p Ve}{kT}}\right] - 1\right) + \frac{z_{Nd} Nd_{ZnO} Ve}{kT}\right]} \tag{S12}$$

Applying boundary conditions S10 and S11 to expression S7 during integration yields the following expression for the potential gradient in the DI-H_2O:

$$\frac{dV}{dx} = \sqrt{-\frac{2kT}{\epsilon_0 \epsilon_{ZnO}}\left[\left(n_b\left[e^{\frac{z_n V e}{kT}}\right]-1\right)+\left(p_b\left[e^{\frac{z_p V e}{kT}}\right]-1\right)\right]} \tag{S13}$$

Up to this point, the derivation of the potential profile in the ZnO (Eq. S12) and DI-H_2O (Eq. S13) have remained independent from one another. However, the electrical potential at the heterojunction only exists because the materials have exchanged mobile charges in order to come to equilibrium with each other. In order to physically couple the ZnO and H_2O systems, two conditions are applied:

1. The electric field at the interface between the ZnO and H_2O must have the same magnitude and direction when calculated from both the ZnO or H_2O side:
$$\left(\frac{dV_{ZnO}}{dx}\right)_{x=0} = \left(\frac{dV_{H_2O}}{dx}\right)_{x=0} \tag{S14}$$
2. The total charge of the system must be:
$$Q_{ZnO} + Q_{Piezo} = Q_{H_2O} \tag{S15}$$

Where Q_{ZnO} and Q_{H_2O} are the net charge in the ZnO and H_2O, respectively. Q_{Piezo} is the first instance thus far to introduce a piezoelectric component to our calculation. Q_{Piezo} represents the charge density present at the interface ZnO interface due to the direct piezoelectric effect.

To calculate Q_{Piezo} we assume the linear piezoelectric equation of state applies. In this case, the charge density (Q_{Piezo}) introduced by straining (E) the piezoelectric perpendicular to the (0001) axis will be uniform across the ZnO surface and given by:

$$Q_{Piezo} = (d_{31})(E)(Y) \tag{S16}$$

Where d_{31} is the direct piezoelectric coefficient ($\frac{Coulomb}{N}$) and Y is Young's modulus ($\frac{\mathrm{N}}{\mathrm{m}^2}$).

We assume a simple, planer heterojunction at the interface. Thus, the charge in the medium can be related to the electric field at the interface by the following expression:

$$Q = \epsilon_0 \epsilon_r \left(\frac{dV}{dx}\right)_{x=0} \tag{S17}$$

Combining S15, S16 and S17 yields the final expression for our second coupling condition:

$$\epsilon_0 \epsilon_{ZnO}\left(\frac{dV_{ZnO}}{dx}\right)_{x=0} + (d_{31})(E)(Y) = \epsilon_0 \epsilon_{H_2O}\left(\frac{dV_{H_2O}}{dx}\right)_{x=0} \tag{S18}$$

Taken together, expressions S14 and S18 couple the physical phenomena occurring in the ZnO (Eq. S12) and DI-H_2O (Eq. S13) systems.

In order to stitch the potential profiles generated by integrating Eq. 12 and Eq. 13 together into a single, cohesive picture (e.g. Figure 1 in the main text), it is necessary to track the potential change as the calculations move from one medium to the next.

In our experiments there are four potentials (referenced to vacuum) that must be stitched together, these potentials include: V1, the bulk potential of ZnO ($V_{EF_{ZnO}} \pm V\ vs.SCE$); V2, the potential at the interface between ZnO and $Ni(OH)_2$;V3, the potential at the interface between $Ni(OH)_2$ and DI-H_2O; and V4, the bulk potential of DI-H_2O ($V_{EF_{H2O}}$). These potentials are schematically represented in figure S7.

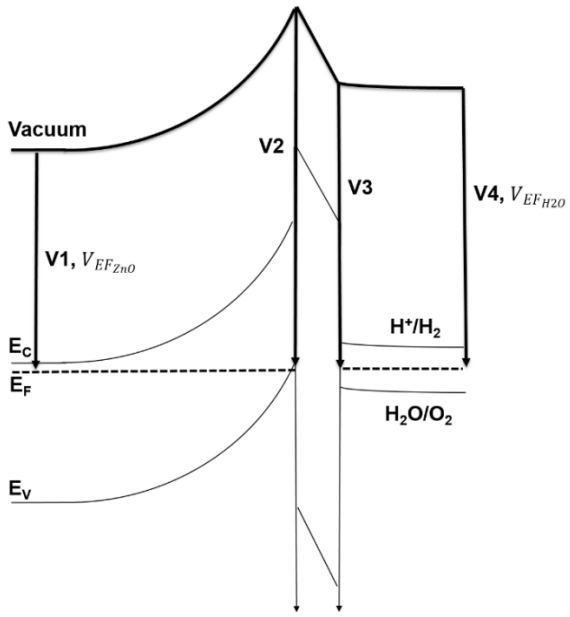

Figure S7. Energy diagram of the ZnO/$Ni(OH)_2$/DI-H_2O heterojunction (with piezoelectric charge present at the ZnO/$Ni(OH)_2$ interface). V1, V2, V3 and V4 denote potentials that define the interfaces between materials and thus need to be combined when generating band diagrams.

The $Ni(OH)_2$ layer is taken as a perfect insulator. Thus, the voltage change between V2 and V3 is equal to the electric field inside the $Ni(OH)_2$ layer ($\left(\frac{dV_{ZnO}}{dx}\right)_{x=0} = \left(\frac{dV_{H_2O}}{dx}\right)_{x=0}$)multiplied by the $Ni(OH)_2$ thickness (Eq. S19).

$$V3 = V2 - \frac{(Q_{ZnO} + Q_{Piezo})}{(\mathrm{Ni(OH)_2\ Thickness})\epsilon_{\mathrm{Ni(OH)_2}}}$$

The values of material properties used in the calculation are aggregated in Table S1.

Table S1. Parameters used and calculated concentrations of various ions from Eq. S2 assuming no physical size of ions.

Material	ϵ_r	$d_{31}(\frac{Coulomb}{N})$	*Thickness*	$V_{EF_{Bulk}}$ (eV *vs* Vacuum)	$Nd\ (\frac{ions}{m^3})$	$n_b(\frac{ions}{m^3})$	$p_b(\frac{ions}{m^3})$	$Y(\frac{N}{m^2})$
ZnO	8.7	-3.3*10^-12	$infinite\ (>100nm)$	-4.2 (at pH 7)	8*10^237	8*10^23	Mass action*	150*10^9
Ni(OH)$_2$	3.425	-	$(varied)$	-	-	-	-	-
H$_2$O	80	-	$infinite$ (>8 μm)	-4.642	-	$6.022 \ldots \times 10^{19}$	$6.022 \ldots \times 10^{19}$	-

*Concentration of holes at every location was determined by law of mass action.

*Bulk concentration of charges in H_2O was set to equilibrium concentration of hydronium and hydroxyl ions at pH = 7.

To calculate the potential profiles when electrolyte Na_2SO_3 was added to solution, Equations S5 and S7 were changed to reflect the addition of Na^+ and SO_3^{2-} to the expression of charge density. CV measurement of electrolyte Na_2SO_3 solution revealed a strong oxidation peak (SO_3^{2-} oxidation) at -4.831V vs Vacuum, this potential was well defined and used as the potential of electrolyte solution (V4).

The pH of electrolyte Na_2SO_3 solution was measured after preparation and found to be 10. For systems where the ZnO electrode was directly exposed to the Na_2SO_3 solution, a change of 0.059eV per pH unit was applied to the flat band potential of the electrode. If the ZnO wasn't in contact with solution (because of a $Ni(OH)_2$ coating), the $V_{EF_{Bulk}}$ of ZnO at pH =7 was used. This flat band potential shift is the reason for the discrepancy in total potential difference between ZnO and solution in the two conditions depicted in Figure 1C.

Checking for physically reasonable values

During every step of the calculation, the properties of the physical environment were checked to ensure that physically reasonable quantities were being produced. Of particular concern was ensuring that the atomic density in solution, adjacent to the ZnO/ DI-H_2O or $Ni(OH)_2$/ DI-H_2O interface, never exceeded the atomic density of a condensed phase.

To calculate the maximum charge densities we could physically expect, we modeled the hydrated ions (Na^+, SO_3^{2-}, H^+, and OH^-) as hard spheres and fit them into the maximum packing density possible, the close packing structure. Taking SO_3^{2-} ions as an example, each with a hydration diameter (d) of 4 Å, the maximum 3D packing density possible is given by:

$$\text{Maximum 3D Density} = \frac{Total\ \text{ions}}{\text{Volume}} = \frac{\left(\frac{3}{2}\right)+3+\left(\frac{3}{2}\right)}{\frac{3\sqrt{3}}{2}a^2c} = \frac{6}{\frac{3\sqrt{3}}{2}(d)(2d\sqrt{\frac{2}{3}})} = 2.20971 * 10^{28}\frac{\text{ions}}{m^3} \quad \text{(S4)}$$

Thus, the total of all ion concentrations at the closest approach to the interface must be approximately equal to or less than this atomic density.

$$n_{max} \leq 2.20971 * 10^{28} \frac{ions}{m^3} \quad \text{(S5)}$$

Summing up the concentration of all hydrated ions in solution at the interface means summing up the value from Equation S3 for each ion:

$$\sum n_i = \sum n_i^0 e^{\left(\frac{-z_i e \phi (V3-V4)}{kT}\right)} \quad \text{(S6)}$$

Table S2 displays the atomic density at the ZnO/H_2O interface as a function of strain and insulator thickness. At no point did our model exceed the maximum charge atomic density n_{max}.

Table S2. Concentration of solution ions as a function of insulator thickness, electrolyte concentration and ZnO strain when ZnO is under a bias of 1V vs SCE.

V1 Vs. SCE	NiOH Thickness (nm)	Na_2SO_3 concentration (Molar)	Strain (%)	n_i ($\frac{ions}{m^3}$)
1	0	0	-0.2	5.79473x 10^{24}
1	0	0	0	4.01274x 10^{24}
1	0	0	0.2	2.56275x 10^{24}
1	0	1	-0.2	1.8144x 10^{27}
1	0	1	0	1.81228x 10^{27}
1	0	1	0.2	1.81051x 10^{27}
1	10	0	-0.2	1.56527x 10^{24}
1	10	0	0	1.17801x 10^{24}
1	10	0	0.2	8.07261x 10^{23}
1	10	1	-0.2	1.80879x 10^{27}
1	10	1	0	1.80828x 10^{27}
1	10	1	0.2	1.8078x 10^{27}

Reference

(1) Shi, J.; Starr, M. B.; Xiang, H.; Hara, Y.; Anderson, M. A.; Seo, J. H.; Ma, Z.; Wang, X. Interface Engineering by Piezoelectric Potential in ZnO-Based Photoelectrochemical Anode. *Nano Lett.* **2011**, *11*, 5587-5593.

(2) Shi, J.; Zhao, P.; Wang, X. Piezoelectric-Polarization-Enhanced Photovoltaic Performance in Depleted-Heterojunction Quantum-Dot Solar Cells. *Adv. Mater.* **2013**, *25*, 916-921.